Molecular Docking Studies of Enzyme Inhibitors and Cytotoxic Chemical Entities

Sadia Sultan, Gurmeet Kaur Surindar Singh,
Kamran Ashraf and Muhammad Ashraf

Additional information is available at the end of the chapter

Abstract

Docking is a powerful approach to perform virtual screening on large library of compounds, rank the conformations using a scoring function, and propose structural hypotheses of how the ligands inhibit the target, which is invaluable in lead optimization. Using experimentally proven active compounds, detailed docking studies were performed to determine the mechanism of molecular interaction and its binding mode in the active site of the modeled yeast α-glucosidase and human intestinal maltase-glucoamylase. All active ligands were found to have greater binding affinity with the yeast α-glucosidase as compared to that of human homologs, intestinal, and pancreatic maltase, by an average value of ~-1.3 and ~-0.8 kcal/mol, respectively. Thirty quinoline derivatives have been synthesized and evaluated against β-glucuronidase inhibitory potential. Twenty-four analogs, which showed outstanding β-glucuronidase activity, have IC_{50} values ranging between 2.11 ± 0.05 and 46.14 ± 0.95 μM than standard D-saccharic acid 1,4-lactone ($IC_{50} = 48.4 \pm 1.25$ μM). Structure activity relationship and the interaction of the active compounds and enzyme active site with the help of docking studies were established. In addition, Small series of morpholine hydrazones synthesized to form morpholine hydrazones scaffold. The *in vitro* anti-cancer potential of all these compounds were checked against human cancer cell lines such as HepG2 (Human hepatocellular liver carcinoma) and MCF-7 (Human breast adenocarcinoma). Molecular docking studies were also performed to understand the binding interaction.

Keywords: docking studies, α-glucosidase inhibitors, cedryl acetate, quinoline, β-glucuronidase inhibitors, morpholine hydrazone

1. Introduction

Due to the current problems and complicated challenges faced by medicinal chemists docking is a most demanding and efficient discipline in order to rational design new therapeutic agents for treating the human disease. Previously, the strategy for discovering new drugs consisted of taking a lead structure and developing a chemical program for finding analog molecules exhibiting the desired biological properties, the whole process involved several trial and error cycles patiently developed and analyzed by medicinal chemists utilizing their experience to ultimately select a candidate analog for further development. The entire process when looked at today, conceptually inelegant. These days picture are quite reverse after the emergence of computational chemistry discipline in science world. The concepts used in three-dimensional (3D) drug design are quite simple. New molecules are conceived either on the basis of similarities with known reference structures or on the basis of their complementarity with the 3D structure of known active sites. Molecular modeling is a discipline that contributes to the understanding of these processes in a qualitative and sometimes quantitative way [1, 2].

In this chapter we have presented a brief introduction of the available molecular docking methods, and their development and applications in drug discovery especially for synthetic and bio-transformed derivatives.

2. Quantum mechanical calculations and molecular docking studies of α-glucosidase inhibitors

Inhibitors of a-glucosidase regarded as a convincing therapeutic target in the development of drugs against diseases such as obesity, diabetes, HIV, and cancer [3, 4]. In this connection, few synthetic a-glucosidase inhibitors (AGI's), such as acarbose, miglitol, and voglibose are in use since last two decades. Among the six drug classes for the management of diabetes mellitus (DM), α-glucosidase inhibitors are one of them. These inhibitors are quite target specific as they act in the intestine locally, in contrast to other oral anti-hyperglycemic drugs, which in addition, alter certain biochemical processes in the human body [5]. Therefore, discovery and development of novel α-glucosidase inhibitors are urgently needed.

2.1. Cedrol, cedryl acetate: microbial transformed metabolites

Development of novel α-glucosidase inhibitors requires screening of a large number of compounds. Cedryl acetate (**1**) and cedrol (**2**) are examples of newly identified α-glucosidase inhibitors that exhibit potent inhibitory activity. The most potent compound one was selected for microbial transformation and the transformed products were screened for the same activity. We successfully identified several α-glucosidase inhibitors that are more potent than acarbose [6]. However, this was the first report describing the α-glucosidase inhibitory activity of cedrol (**2**), cedryl acetate (**1**), [7] and some of the transformed products of cedryl acetate including 10β-hydroxycedryl acetate (**3**), 2α, 10β-dihydroxycedryl acetate (**4**), 2α-hydroxy-10-oxocedryl

acetate (**5**), 3α,10β-dihydroxycedryl acetate (**6**), 3α,10α-dihydroxycedryl acetate (**7**), 10β,14α–dihydroxy cedryl acetate (**8**), 3β,10β-cedr-8(15)-ene-3,10-diol (**9**), and 3α, 8β, 10β -dihydroxycedrol (**10**) as mentioned in **Figure 1**. Compounds one, two, and four showed α-glucosidase inhibitory activity whereby one was more potent than the standard inhibitor, acarbose, against yeast α-glucosidase.

The structures have been also optimized computationally at Hartree-Fock (HF) level of theory using valence triple-zeta plus diffuse and polarization functions (6–311++G*) basis sets for H, C, N, and O atoms to get insight into the 3D structure of these metabolites. GAMESS package [8] has been used for all quantum chemical calculations. Molecular docking studies have been also performed to delineate the ligand-protein interactions at molecular level using autodock vina programs [9]. Avogadro [10], Gabedit [11], VMD [12], and Chimera [13] have been used for the structure building, analysis, and visualization for our calculations.

2.2. α-Glucosidase inhibitory activity

Compounds one, two, four, and six were tested for inhibition of the α-glucosidase enzyme. For the first time, the cedrol (**2**) and cedryl acetate (**1**) demonstrated α-glucosidase inhibitory with the latter being more potent than the former. This is possibly due to the presence of an Ac group at C (8). Overall compounds one, two, and four showed more than or comparable activity to the standard inhibitors (**Table 1**). Apparently, the polar OH group lowers the inhibitory activity toward the enzyme, as observed in compounds four and six (inactive) in comparison to one.

2.3. Geometry optimization

The biological activity of ligands is a function of their 3D structures. Thus, it is crucial to have an accurate description of the ligand in 3D space. Hartree-Fock (HF) approach have been used
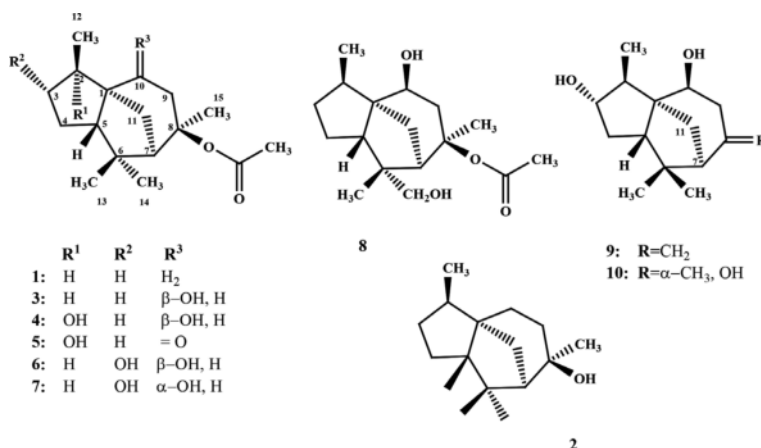

	R¹	R²	R³
1:	H	H	H₂
3:	H	H	β–OH, H
4:	OH	H	β–OH, H
5:	OH	H	= O
6:	H	OH	β–OH, H
7:	H	OH	α–OH, H

9: R=CH₂
10: R=α–CH₃, OH

Figure 1. Structure of cedryl acetate and its microbial derivatives.

Compound	IC50* (in mM ± S.E.M)	Binding energy in kcal/mol (Yeast a-glucosidase)	Binding energy in kcal/mol (Human maltase glucoamylase)		Binding energy in kcal/mol (Human pancreatic amylase; 1 U33.pdb)
			C-terminal domain (3TOP.pdb)	N-terminal domain (3L4T.pdb)	
1	94 ± 15	−8.4	−6.9	−6.5	−7.9
2	130 ± 15	−7.4	−6.6	−6.2	−7.9
4	690 ± 16	−7.9	−6.3	−7.1	−7.6
6	Inactive	−8.2	−6.4	−6.5	−7.6
Acarbose	780 ± 20	—	—	—	—
Deoxynojirimycin	425.6 ± 8.14	—	—	—	—

Table 1. α-Glucosidase inhibitory activity of compounds **1**, **2**, **4** and **6** with their predicted binding energies in the active sites of yeast and mammalian α-glucosidases.

to obtain the structural details of all metabolites that were probed through the geometry optimization in the gaseous-phase with valence triple-zeta plus diffuse and polarization functions (6–311++G*) basis sets. We found in all the compounds studied, the distance of the bond between C and OH is 1.421 Å. The optimized geometry of these compounds also, showed a short length of carbonyl groups (C=O and COC=OCH3) distance of 1.208 Å. However, the bond order was slightly higher by a value of 0.11 in the case of C=O as expected. The carbon–oxygen bond in C-OCOCH$_3$ was slightly larger as compared to that in CO-COCH3 (1.402 and 1.338 Å, respectively) due to a lower bond order by a value of 0.233. The presence of acetate group (-O-CO-CH3) in the molecule was lowered the dipole moment of the molecule as could be seen in **Table 2**. These compounds with a low dipole moment seem to be most active. However, due to limited experimental inhibitory assay data, it was difficult to make a generalize conclusion.

Compound	Dipole (Debye)
1	2.03
2	3.03
3	2.87
4	3.87
5	5.07
6	3.90
7	4.09
8	3.93
9	2.65
10	6.01

Table 2. Dipole moment of metabolites calculated at HF/6–311++G* level of theory and basis sets.

2.4. Molecular docking studies

The most ideal is to obtain the orientation of ligand in 3D space into the protein binding site for determination of ligand activity. The ligand-protein binding mode and interaction are a very crucial to understand the catalytic activity. This modeled protein has been used as our target protein. In Addition, to elucidate their binding activity with mammalian α-glucosidase, we performed molecular docking studies of the human intestinal and pancreatic maltase glucoamylase with the active compounds. We found no significant difference in the binding affinity of active ligands with yeast α-glucosidase and the human pancreatic maltase glucoamylase. However, some differences in the binding energy were observed when ligands bind with the human intestinal maltase (**Table 1**). The structural changes in the binding sites of these proteins are
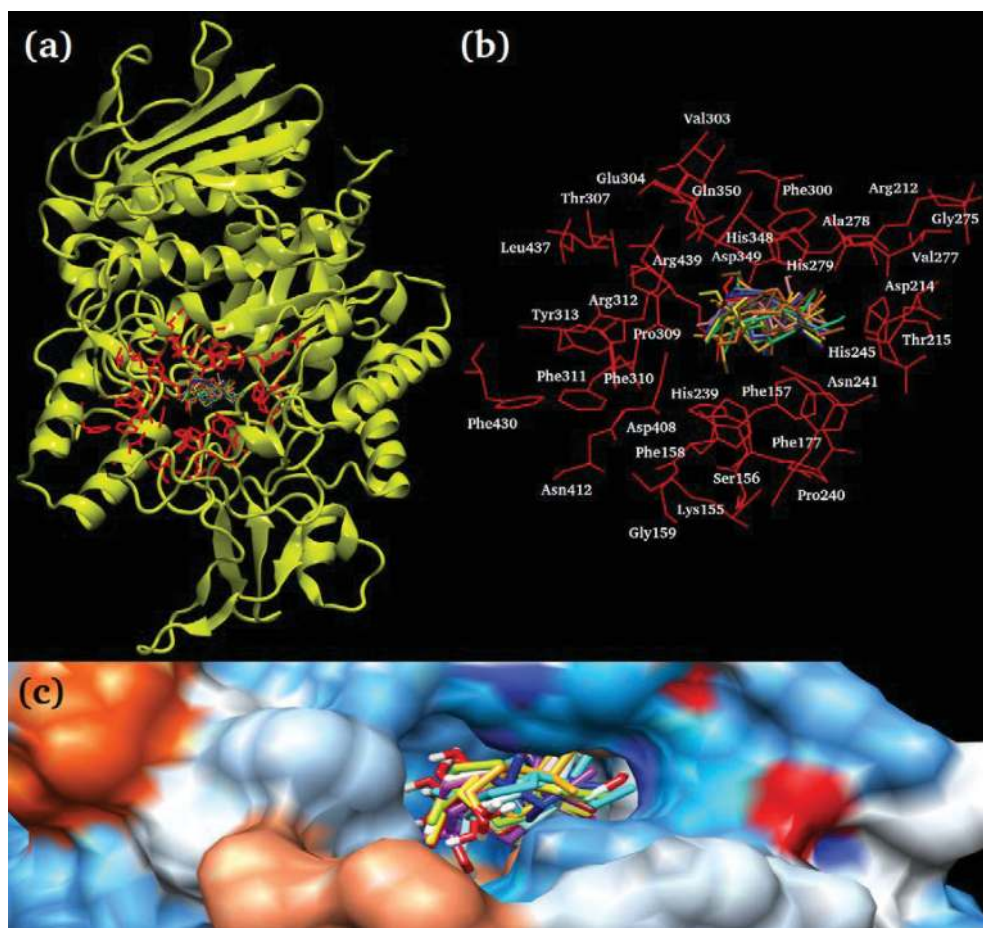
Figure 2. (a) Homology model of the yeast α-glucosidase (yellow color) showing the ligand cluster (variable color; licorice) into the binding site. The red color indicates the amino acid residues (labeled in white) surrounding the binding site (b). The lower picture (c) displays the binding site cavity with the ligand cluster.

postulated to be the cause of this less affinity of ligands toward intestinal maltase as compared to the yeast α-glucosidase. **Figure 2a** shows the homology model of the yeast α-glucosidase with the ligand cluster into the binding site. **Figure 2b** displays the close view of the binding site with the best predicted orientation of ligands **1–15,** obtained from the molecular docking studies, almost overlapping with each other to form a cluster. The amino acid residues forming the binding site cavity have been labeled in white. The cavity can be clearly visualized when the protein is shown with the surface model as depicted in **Figure 2c**.

Figure 3 displays the interactions of individual metabolites one, two, four, and six with the yeast α-glucosidase protein. Polar amino acid residues, that is, Asp349 and Arg439 have strong H-bonding with the acetate group of the ligand. Cedryl acetate (**1**) exhibits the strongest binding affinity with the protein as inferred by its lowest binding energy (−8.4 kcal/mol), the values are given in **Table 1**. Compound one had the lowest *IC50* of 94 ± 15 μM, which makes it
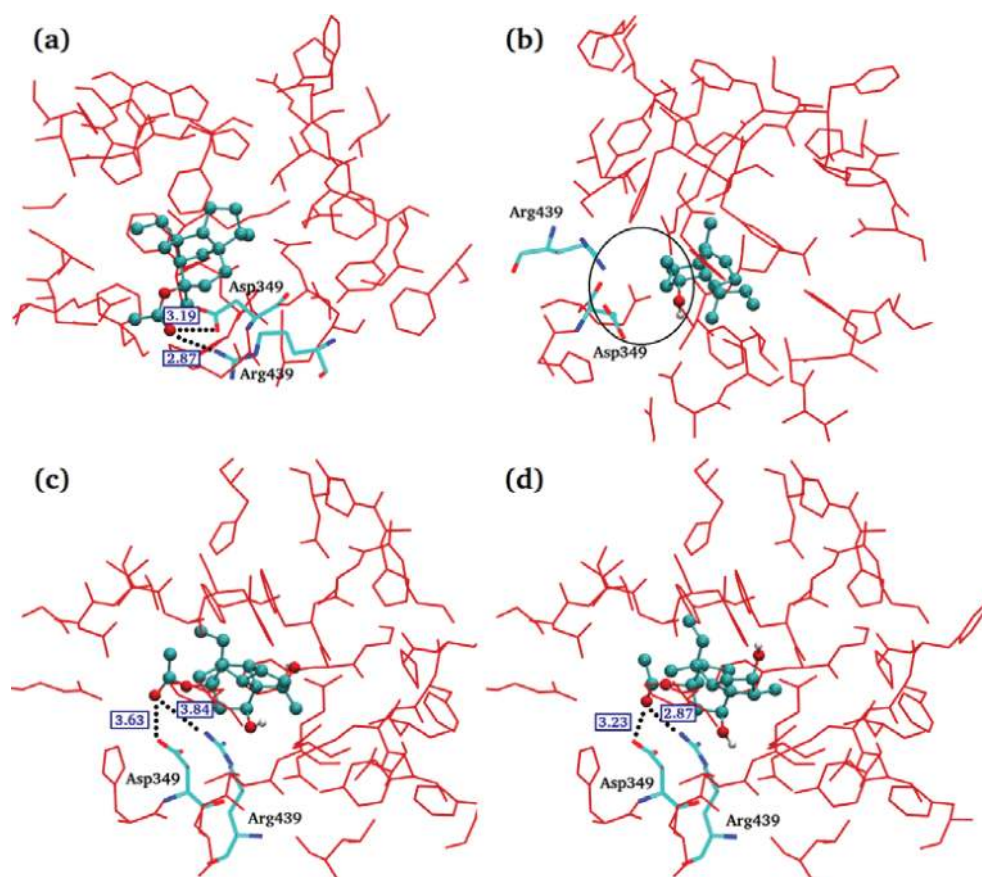
Figure 3. Ligand-protein interaction studies of compounds (a) 1, (b) 2, (c) 4, and (d) 6. The hydrogen bonds are shown as black dotted lines. The H-bond distances in Å are given in boxes. The amino acid residues in the binding pockets are indicated as red.

in agreement with the enzymatic assay. The metabolite **2**, showed no interaction with the residues. The acetate group of metabolite two has been hydrolyzed to form hydroxyl group that may play a partial role in its low activity (**Figure 3b**) as compared to the compound one. Metabolites four and six are acetylated and they do form H-bonds with Asp349 and Arg439, thereby showing a good ligand-protein binding energy, however, their activity is dramatically lowered or diminished as compared to compound one. This attenuate activity of metabolites four and six may be associated with their high-polarity arising from the introduction of two hydroxyl groups into the rings, partially due to the fact that the neighboring residues around -OH are slightly hydrophobic in nature.

3. Molecular docking studies of novel quinoline derivatives as potent β-glucuronidase inhibitors

Glucuronidase has been used in numerous biotechnology and research applications. Glucuronidase as a gene has been studied as a positive selection marker for transformed plants, bacteria, and fungi carrying glucuronidase gene [14, 15]. It is also widely has been used for the structural investigations of proteoglycans and for research purposes in many diagnostic research laboratories [16].

3.1. Novel quinoline derivatives as potent β-glucuronidase inhibitors

Quinoline is an aromatic compound having an aza-heterocyclic ring. It possesses a weak tertiary base that can undergo both nucleophilic and electrophilic substitution reactions. The quinoline moiety is present in several pharmacologically active compounds as it does not harm humans, when it is orally absorbed or inhaled.

Various classes of compounds that showed considerable potential as β-glucuronidase inhibitors involved benzothiazole, bisindolylmethanes, bisindolylmethane-hydrazone, benzimidazole, unsymmetrical heterocyclic thioureas, 2,5-disubtituted-1,3,4-oxadiazoles with benzimidazole backbone, and benzohydrazone–oxadiazole [17]. In continuation of this work our study identified novel series of potent β-glucuronidase inhibitors of quinoline for further investigation [18].
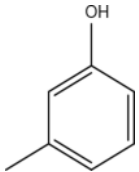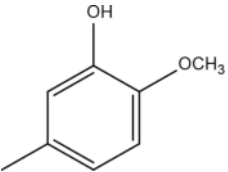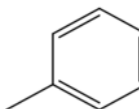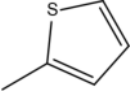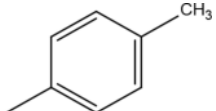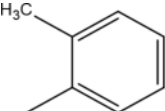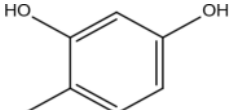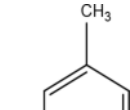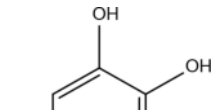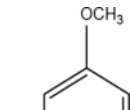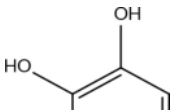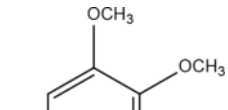
3.2. β-Glucorinadase inhibitory activity

Thirty analogs of quinoline were synthesized, which have varied degree of β-glucorinadase inhibition ranging in between 2.11 ± 0.05 and 80.10 ± 1.80 μM, when compared with the standard inhibitor D-saccharic acid 1,4 lactone having IC$_{50}$ value 48.4 ± 1.25 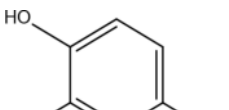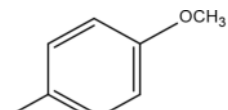μM. Out of these thirty analogs, twenty four analogs 1–30 showed outstanding β-glucorinadase inhibitory potential with IC$_{50}$ values (**Table 3**) analogs 17, 20, 21, and 27–29 showed good β-glucorinadase inhibitory potential. The structure–activity relationship studies suggested that the β-glucuronidase inhibitory activities of this class of compounds are mainly dependent upon the substitutions on the phenyl ring.
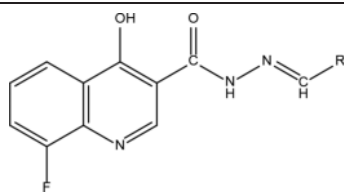
Quinoline hydrazones (1-30)

No	R	$IC_{50} \pm SEM^a$ [μM]	No	R	$IC_{50} \pm SEM^a$ [μM]
1		18.40 ± 0.45	16		16.60 ± 0.55
2		42.25 ± 0.80	17		78.90 ± 1.50
3		24.20 ± 0.40	18		44.10 ± 0.70
4		9.20 ± 0.30	19		19.40 ± 0.90
5		37.01 ± 0.70	20		68.38 ± 1.25
6		26.30 ± 0.50	21		49.38 ± 0.90
7		38.50 ± 0.80	22		9.60 ± 0.20
8		6.70 ± 0.25	23		8.30 ± 0.20

#	Structure	IC50	#	Structure	IC50
9	OH	18.10 ± 0.40	24	OH, OCH3	18.00 ± 0.30
10	OH	9.60 ± 0.20	25	S	22.30 ± 0.45
11	CH3	46.14 ± 0.95	26	H3C	38.50 ± 0.80
12	HO, OH	3.10 ± 0.10	27	CH3	51.00 ± 1.25
13	OH, OH	2.11 ± 0.05	28	OCH3	80.10 ± 1.80
14	HO, OH	5.01 ± 0.20	29	OCH3	69.40 ± 1.30
15	OH, HO	2.60 ± 0.05	30	OCH3, OCH3	46.10 ± 0.85
	D-Saccharic acid 1,4-lactone	48.4 ± 1.25			

ª IC50 values are expressed as mean ± standard error of mean.

Table 3. Different quinoline derivatives and their β-glucuronidase activity.

The most potent inhibition was noted in analog 13 that have hydroxy groups at 3, 4-positions on the phenyl part. Making comparison of analog 13 having IC$_{50}$ value 2.11 ± 0.05 μM with other dihydroxy analogs such as 12, 14, and 15 having IC$_{50}$ values 3.10 ± 0.10, 5.01 ± 0.20, and

2.60 ± 0.05 μM, respectively, analog 13 was found to be superior than other. In analog 13 the two hydroxy groups are present at *meta-para* position while in analog 12 the two hydroxy groups are present at *ortho-para* positions, in analog 14 the two hydroxy groups are present at *ortho-meta* positions, and in analog 15 the two hydroxy groups are present at *ortho-meta* positions. The little bit difference in the activity of these analogs may be due to the difference in position of the substituents on the phenyl part.

Similarly, effect of substituent position was also observed in other analogs such as 4, 5, and 6 having fluoro group. If we compare analog four, a *ortho* analog, having IC_{50} value 9.20 ± 0.30 μM with analog five, a *meta* analog, and six, a *para* analog having IC_{50} values 37.01 ± 0.70 and 26.30 ± 0.50 μM, respectively. In analog four the fluoro group is present at *ortho* position while in analog five the floro group is present at *meta* position and in analog six the floro group is present at *para* position. These three analogs demonstrated minute differences in their activity possibly due to the difference in the position of the substituents of the phenyl section. This was also observed in monohydroxy analogs. From these findings, we concluded that the factors that influence the inhibitory potentials of these analogs include the nature, position, and the number of substituents.

3.3. Docking studies

Molecular docking is a useful tool to obtain data on binding mode and to validate experimental results of active derivatives within the active site of β-D-glucuronidase. By using X-ray crystal structure of the human β-glucuronidase enzyme at 2.6 Å resolution (PDB ID: 1BHG) [19], it can be used to identify predict the binding modes involved in the inhibition activity.

Utilizing docking approach, we identified the stable binding mode of six most active compounds (8, 12–15, and 23) that was further used in characterizing their inhibitory activity. Compounds with the most stable binding conformation suggest to strongly alignment to the core of β-glucuronidase. In **Figure 4** shows that the quinolone moiety of these active compounds are oriented toward the active pocket and share some common interaction with catalytically important amino acids such as Glu450, Glu541, and Tyr504.

We predict that the hydrogen bonding interaction between the hydroxyl at C-4 of quinoline moiety and Glu451 plays a vital role. According to the docking result compound **13** (**Figure 5**),
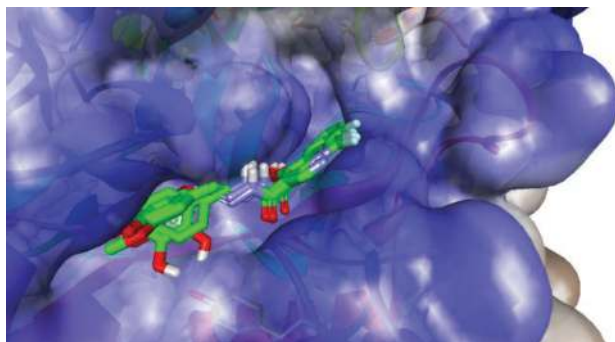

Figure 4. Active compounds aligned well into the binding cavity of β-glucuronidase enzyme.
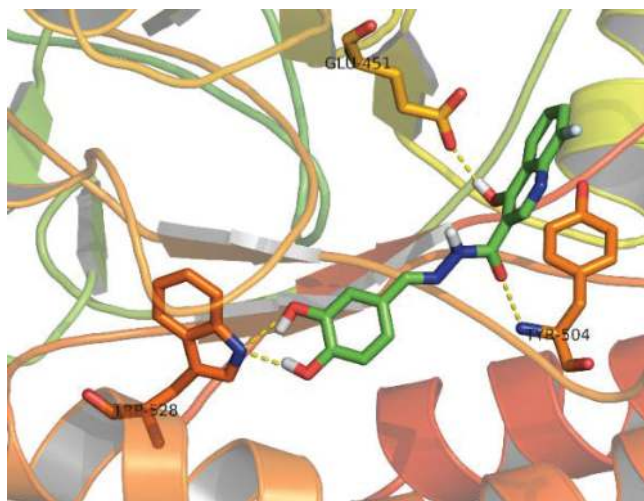
Figure 5. Best binding position of compound **13** in active pocket of β-glucuronidase enzyme.

was found to be to most active compound in this series, because of the hydroxyl (OH) at C-4 involved in hydrogen bonding with Oε2 of Glu451 side chain (1.99 Å). The complex is stabilized by π-donor hydrogen bond formation between the benzene ring on quinoline moiety and with hydroxyl (OH) of Tyr508 (3.73 Å). Two interactions were detected in hydrazone linkage between carboxamide and the surrounding residues. The hydrazone carbonyl (C=O) oxygen linked by a hydrogen bonding with the nitrogen on the backbone of Tyr504 (2.77 Å), another hydrogen bond forms between the NH group and the oxygen on side chain of Asn484 with a bond length of 3.10 Å. The two hydroxyls on the benzylidene moiety at *meta* positions also, involved in hydrogen bonds with indole nitrogen at Trp528 backbone having a distance of 2.11 and 1.99 Å, respectively.

Compound 15 showed that hydroxyl (OH) at C-4 of quinoline moiety for compound formed hydrogen bonding with Oε2 of Glu451 side chain at a longer distance (2.24 Å) as compared to previous compound (**Figure 6**). In this compound the quinoline benzene rings on forms a π-donor hydrogen bond with hydroxyl (OH) of Tyr508 at (3.96 Å). It was also observed that hydrazone linkage was oxygen of carbonyl (C=O) interacts with side chain of Tyr504 through a hydrogen bond at a distance of 2.80 Å. Both form hydrogen bonds were formed between hydroxyls at *ortho* and *meta* position on the benzylidene moiety and nitrogen of indole backbone of Tyr508 at a distance of 2.19 and 1.99 Å, respectively. Compound 15 was found to be a second most active inhibitor.

In third most active compound 12 (**Figure 7**), it was observed that hydroxyl (OH) at Carbon no 4 exhibited hydrogen bonding with Oε2 of Glu451 side chain with a distance of 2.11 Å. On the other hand we noted that a more stable π-donor hydrogen bond with hydroxyl (OH) of Tyr508 at (3.77 Å) and benzene ring on quinoline moiety when compared with derivative 14. Docking studies also showed the hydrazone linkage interaction of oxygen of carbonyl (C=O) with side chain of Tyr504 through a hydrogen bond with length of 2.99 Å. There is also a hydrogen
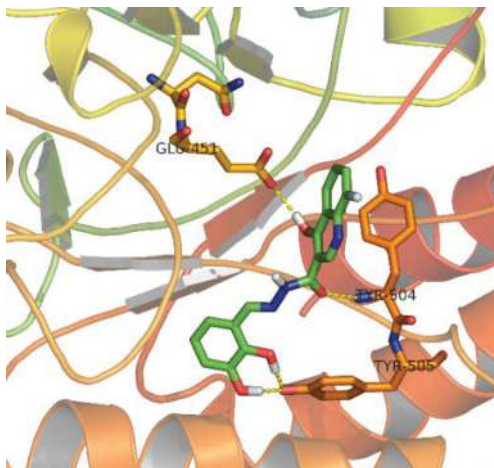
Figure 6. Binding positions of compound 15 in an active pocket of the β-glucuronidase enzyme.
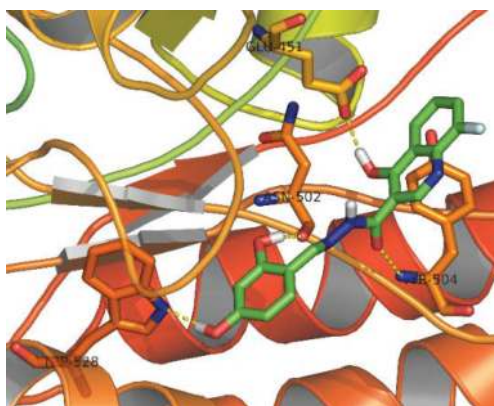

Figure 7. Binding position of compound 12 in an active pocket of the β-glucuronidase enzyme.

bonding of hydroxyl at *ortho* position on the benzylidene with the oxygen of Asn502 (1.87 Å), while the other another hydrogen bonding of hydroxyl at *para* position on the benzylidene with the nitrogen of indole backbone of Trp528 (1.89 Å).

4. Morpholine hydrazone scaffold: synthesis, anticancer activity, and docking studies

Cancer is a broad term to describe a disease that characterized by the uncontrolled proliferation of cells resulting from the disruption or dysfunction of regulatory signaling pathways that

are normally under tight control [20, 21]. In modern life, cancer is one of the big health killers. According to the American Association for cancer research (AACR) cancer progress report 2013, it expected that 580,350 Americans would die from the various type of cancer in the same year. Luckily, ultimate evolution has made against cancer. Approximately, from 1990 to 2012 almost 1,024,400 lives saved [22].

Currently chemotherapy is an ultimate clinic treatment to repel cancer [23]. Cisplatin drug has been commonly used in cancer treatment for decades [24, 25]. Though, its clinical value tends to be inadequate by the abrupt increase of drug resistance or new side effects [26]. Consequently, the exploration of unusual chemotherapeutic agents has sparked the great attention of scientists from varied disciplines.

The morpholine scaffold has been found to be an outstanding pharmacophore in medicinal chemistry and a number of molecules having morpholine skeleton are the clinically approved drugs [27]. N-substituted morpholines are used in the treatment of inflammatory diseases, such as migraine and asthma [28]. Morpholines derivatives have reported to possess activity such as platelet aggregation inhibitors, anti-eme-tics, and bronchodilators [29]. Morpholine analogs establish a new antifungal chemical entity not allied with other presently available medications with anti-fungal potential. The benefit in synthesizing morpholine analogs resides in the fact that these molecules offer chlorohydrates that are water soluble for pharmacological assays [30, 31].

Recently, we have reported synthesis, characterization, anti-cancer activity, and molecular docking studies of morpholine derivatives [32]. A small series of morpholine hydrazones synthesized by treating 5-morpholinothiophene-2-carbaldehyde with different aryl hydrazides to form morpholine hydrazones scaffold (**1–17**) (**Table 4**). The *in vitro* anti-cancer potential of all these compounds were checked against human cancer cell lines such as HepG2 (Human hepatocellular liver carcinoma) and MCF-7 (Human breast adenocarcinoma). Analogs **13** had similar substantial cytotoxic effects toward HepG2 with IC_{50} value 6.31 ± 1.03 μmol/L when compared with the standard doxorubicin (IC_{50} value 6.00 ± 0.80 μmol/L); while compounds five, eight, and nine showed potent cytotoxicity against MCF-7 with IC_{50} value 7.08 ± 0.42, 1.26 ± 0.34, and 11.22 ± 0.22 μmol/L, respectively, when compared with the standard Tamoxifen (IC_{50} = 11.00 ± 0.40 μmol/L). Molecular docking studies also performed to understand the binding interaction.

4.1. In vitro anti-cancer activity

All synthesized analogs (**1–17**) were screened against two human cancer cell lines, human breast carcinoma (MCF-7) and human liver carcinoma (HepG2). The potentials of these analogs calculated in IC_{50} value shown in **Table 5**. Among the series 10 compounds showed potential against HepG2 and six compounds showed potential against MCF-7.

Among them compound eight was found to be the excellent inhibitor against MCF-7 with IC_{50} value 1.26 ± 0.34 μmol/L, which is more potent than the standard inhibitor Tamoxifen (IC_{50} = 11.00 ± 0.40 μmol/L). Secondly, the compound five was found to be more potent with IC_{50} value 7.08 ± 0.42 μmol/L almost two fold better than the standard. The analogs such as
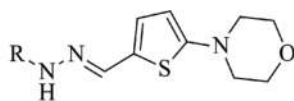
S.NO.	R	S.NO.	R
1		10	
2		11	
3		12	
4		13	
5		14	
6		15	
7		16	
8		17	
9			

Table 4. Various analogs of morpholine.

S. No.	HepG2	MCF-7	S. No.	HepG2	MCF-7
2	—	30.0 ± 1.00	9	40.0 ± 0.93	11.22 ± 0.22
4	7.94 ± 7.94	—	11	19.95 ± 1.31	41.67 ± 1.62
5	19.95 ± 0.63	7.08 ± 0.42	12	31.0 ± 2.26	—
6	12.59 ± 1.22	—	13	6.31 ± 1.03	—
7	20.0 ± 0.32	14.13 ± 1.42	14	56.23 ± 0.56	—
8	—	1.26 ± 0.34	15	15.85 ± 0.82	—
Doxorubicin	6.00 ± 0.80	—			
Tamoxifen	—	11.00 ± 0.40			
Cisplatin	12.00 ± 0.33	15.00 ± 0.80			

Table 5. Anti-cancer activity data (IC_{50} values in µmol/L) of morpholine derivatives (1–17).

two, seven, nine, and 11 also showed potent inhibition for this cell line, while remaining analogs found to be completely in active.

Compound 13 showed potent inhibition against HepG2 with IC_{50} value 6.31 ± 1.03 µmol/L when compared with the standard Doxorubicin (IC_{50} value 6.00 ± 0.80 µmol/L). Compound four and six were found second and third most active analogs among the series with IC_{50} value 7.94 ± 7.94 and 12.59 ± 1.22 µM, respectively. Other analogs such as five, seven, nine, 11, 12, 14, and 15 also showed good to moderate potential.

Molecular docking studies were performed to investigate the binding mode of the active compounds.

4.1.1. Molecular docking analysis of morpholinothiophene hydrazone compounds

The molecular docking procedure was widely used to predict the binding interaction of the compound in the binding pocket of the enzyme. The 3D crystal structure of the topoisomerase II enzyme (PDB id: 4FM9) was retrieved from the protein data bank. All the ions and water molecules removed and the hydrogen atoms added to the enzyme by the 3D protonation using the Molecular Operating Environment (MOE) software. The target enzymes were then energy minimized by the default parameters of the MOE for the stability and further assessment of the enzyme. The structures of the analogs of the morpholinothiophene hydrazone compounds built in MOE and energy minimized using the MMFF94x force field and gradient 0.05. The active site pocket of the enzyme found out by the site-finder implemented in the MOE software. The synthesized compounds docked into the active site of the target enzyme in MOE by the default parameters, that is, placement: Triangle matcher, Rescoring, and London dG. For each ligand, 10 conformations generated. The top-ranked conformation of each compound used for further analysis.

Molecular docking studies predicted the proper orientation of the compound five inside the binding pocket of topoisomerase II enzyme. From the docking conformation of this active compound, we have observed a docking score of **(−11.4975),** which correlates well to the biological activities (IC_{50} = 19.95 ± 0.63 µmol/L in HepG2 and **7.08 ± 0.42** µmol/L in MCF-7
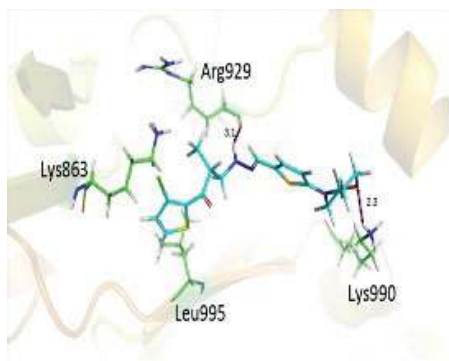
Figure 8. Docking conformations of compound five in the active site of topoisomerase II enzyme.

cell lines). The compound was observed making two interactions with active residues of the active site pocket of the enzyme. The oxygen atom of the morpholine moiety of the compound formed side chain acceptor interaction with the Lys 990 residue of the binding pocket. Arg 929 was observed making the hydrogen bond with the –NH group of the hydrazine moiety of the ligand as shown in the **Figure 8**. The electro-negative nature of Cl, O, and S of the substituent moiety may increase the polarizability of the ligand by electrons withdrawing inductive effect resulting in the enhanced potency and interactions.

5. Conclusion

The molecular docking is now fully recognized and integrated in the research process. In the past the emergence of this new discipline had occasionally encountered some opposition here and there. At presents, the science is mature and there are a growing number of success stories that continuously expand the armory of drug research. Several considerations that can greatly improve the success and enrichment of true bioactive hit compounds are commonly overlooked at the initial stages of a molecular docking study. In this chapter, we tried to cover several of these considerations, including few examples, of molecular docking studies of natural and synthetic analogs of potent α-glucosidase inhibitors, β-glucuronidase inhibitors, and cytotoxicity from our own findings. These molecular studies were performed for different classes of bioactive compounds in order to understand the binding interaction of the active compounds. It was concluded that the nature, position as well as the number of substituents affects the inhibitory potential of these analogs.

Acknowledgements

Author details

Sadia Sultan[1,2,3]*, Gurmeet Kaur Surindar Singh[1,3], Kamran Ashraf[1] and Muhammad Ashraf[4]

*Address all correspondence to: sadiasultan301@yahoo.com; drsadia@puncakalam.uitm.edu.my

1 Faculty of Pharmacy, Universiti Teknologi MARA, Puncak Alam Campus, Bandar Puncak Alam, Selangor Darul Ehsan, Malaysia

2 Atta-ur-Rahman Institute for Natural Products Discovery (AuRIns), Universiti Teknologi MARA, Puncak Alam Campus, Bandar Puncak Alam, Selangor Darul Ehsan, Malaysia

3 Pharmaceutical and Life Sciences Core, Universiti Teknologi MARA, Shah Alam, Shah Alam, Selangor Darul Ehsan, Malaysia

4 Merck Pharmaceutical Private Limited, Karachi, Pakistan

References

[1] Meyer EF, Swanson MS, Williams JA. Pharmacology & Therapeutics. 2000;**85**:113-121

[2] Abraham DJ. Burger's Medicinal Chemistry Drug Discovery. 6th ed. Vol. 12003. pp. 847-900

[3] Pili R, Chang J, Partis RA, Mueller RA, Chrest FJ. A. Passaniti Cancer. Research. 1995;**55**:2920

[4] Zitzmann N, Mehta AS, Carrouée S, et al. Proceedings of the National Academy of Sciences of the United States of America. 1999;**96**:11878

[5] Hitoshi S, Nagao M, Harada T, Nakajima Y, Tanimura-Inagaki K, et al. Journal of Diabetes Investigation. 2014;**23**:206-212

[6] Choudhary MI, Atif M, Shah SAA, Sultan S, Erum S, Khan SN, Atta-ur-Rahman. International Journal of Pharmaceutical Science. 2014;**6**:375-378

[7] Sultan S, Choudhary MI, Nahar Khan S, Fatima U, Ali RA, Atif M, Atta-ur-Rahman, Fatmi MQ. European Journal of Medicinal Chemistry. 2013;**62**:764-770

[8] Trott O, Olson AJ. Journal of Computational Chemistry. 2010;**31**:455-461

[9] Hanwell MD, Curtis DE, Lonie DC, Vandermeersch T, Zurek E, Hutchison GR. Journal of Cheminformatics. 2012;**4**:17

[10] Allouche AR. Journal of Computational Chemistry. 2011;**32**:174-182

[11] Humphrey W, Dalke A, Schulten K. Journal of Molecular Graphics. 1996;**14**:33-38

[12] Pettersen EF, Goddard TD, Huang CC, Couch GS, Greenblatt DM, Meng EC, Ferrin TE. Journal of Computational Chemistry. 2004;**25**:1605-1612

[13] Smith RV, Rosazza J. Journal of Pharmaceutical Sciences. 1975;**64**:1737-1759

[14] Wenzl P, Wong L, Kwang-won K, Jefferson RA. Molecular Biology and Evolution. 2005;**22**: 308-316

[15] Basu C, Kausch AP, Chandlee JM. Biochemical and Biophysical Research Communications. 2004;**320**:7-10

[16] Kuroyama H, Tsutsui N, Hashimoto Y, Tsumuraya Y. Carbohydrate Research. 2001;**333**: 27-39

[17] Khan KM, Rahim F, Halim SA, Taha M, Khan M, Perveen S, Haq Z, Mesaik MA, Choudhary MI. Bioorganic & Medicinal Chemistry. 2011;**19**:4288

[18] Taha M, Sultan S, Nuzar HA, Imran S, Ismail NH, Rahim F, Ullah H. Bioorganic and Medicinal Chemistry. 2016;**4**:3596

[19] Taha M, Ismail NH, Imran S, Ali M, Jamil W, Uddin N, Kashif SM. RSC Advances. 2016;**6**: 3276

[20] Chen WS, Ou WZ, Wang LQ, et al. Dalton Transactions. 2013;**42**:15678-15686

[21] Rahman FU, Ali A, Guo R, et al. Dalton Transactions. 2015;**44**:2166-2175

[22] Sawyers CL, Abate-Shen C, Anderson KC, et al. AACR cancer progress report 2013. Clinical Cancer Research. 2013;**19**:S1-S98

[23] Robert NJ, Diéras V, Glaspy J, et al. Journal of Clinical Oncology. 2011;**29**:1252-1260

[24] Rosenberg B, Van Camp L, Krigas T. Nature. 1965;**205**:698-699

[25] Sak A, Grehl S, Engelhard M, et al. Clinical Cancer Research. 2009;**15**:2927-2934

[26] Galluzzi L, Senovilla L, Vitale I, et al. Oncogene. 2012;**31**:1869-1883

[27] Andrs M, Korabecny J, Jun D, et al. Journal of Medicinal Chemistry. 2015;**58**:41-71

[28] Dugave C, Demange L. Chemical Reviews. 2003;**103**:2475-2532

[29] Arrieta A, Oteagui D, Zubia A, et al. The Journal of Organic Chemistry. 2007;**72**:4313-4322

[30] Polak A. Annals of New York Academy of Sciences. 1988;**554**:221-228

[31] Kerkenaar A. Prous Science Publ., 1987;**1**:523-542. R.G.M.P

[32] Taha M, Shah SAA, Afifi M, Sultan S, Ismail NH. Chinese Chemical Letters. 2017;**28**:607-611